Supplementary Materials

Amide-functionalized copolymer electrolyte with high ionic conductivity and transference number for high-performance lithium metal batteries

Tianlu Ren[1], Jie Zhang[1], Zhiyong Fu[1], Zhenxing Liang[1,*], Kai Wan[1,2,*]

[1]Guangdong Provincial Key Laboratory of Fuel Cell Technology, School of Chemistry and Chemical Engineering, South China University of Technology, Guangzhou 510641, Guangdong, China.
[2]School of Chemical Engineering and Technology, Sun Yat-sen University, Zhuhai 519082, Guangdong, China.

[*]**Correspondence to:** Prof. Zhenxing Liang, Guangdong Provincial Key Laboratory of Fuel Cell Technology, School of Chemistry and Chemical Engineering, South China University of Technology, Guangzhou 510641, Guangdong, China. E-mail: zliang@scut.edu.cn; Prof. Kai Wan, School of Chemical Engineering and Technology, Sun Yat-sen University, Zhuhai 519082, Guangdong, China. E-mail: wank6@mail.sysu.edu.cn

ORCID: Zhenxing Liang (0000-0002-8665-3883), Kai Wan (0000-0003-4689-310X)

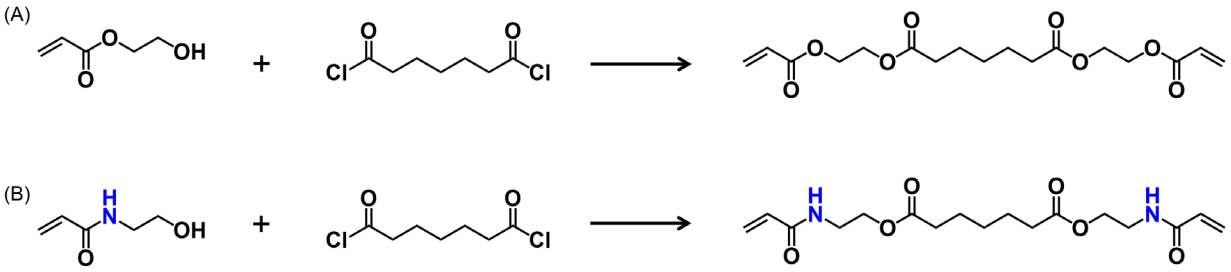

Supplementary Figure 1. Synthesis of (A) DAH and (B) Am-DAH monomers.

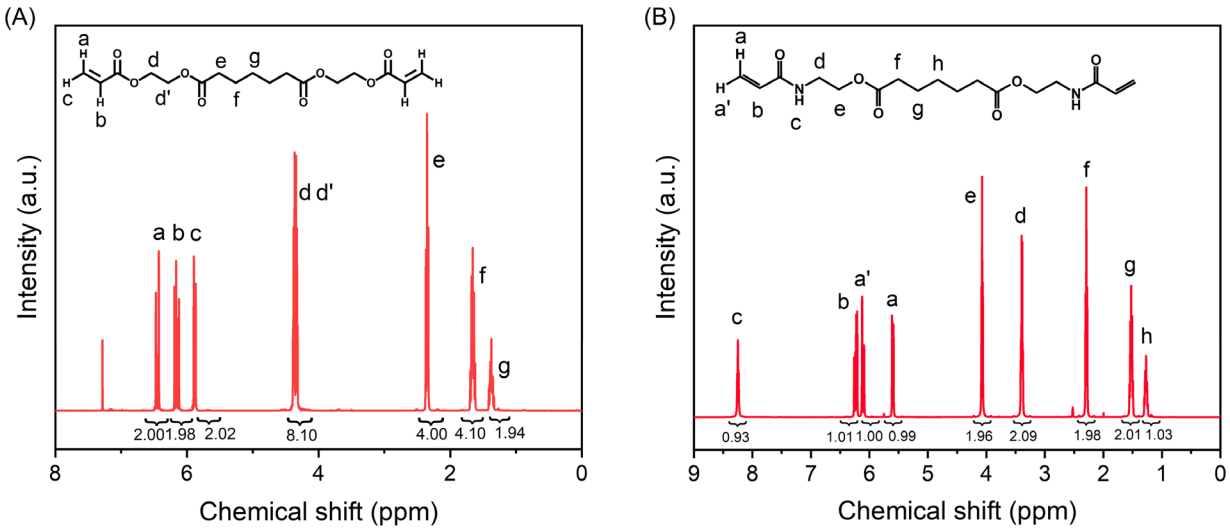

Supplementary Figure 2. ^{1}H NMR spectra of (A) DAH and (B) Am-DAH.

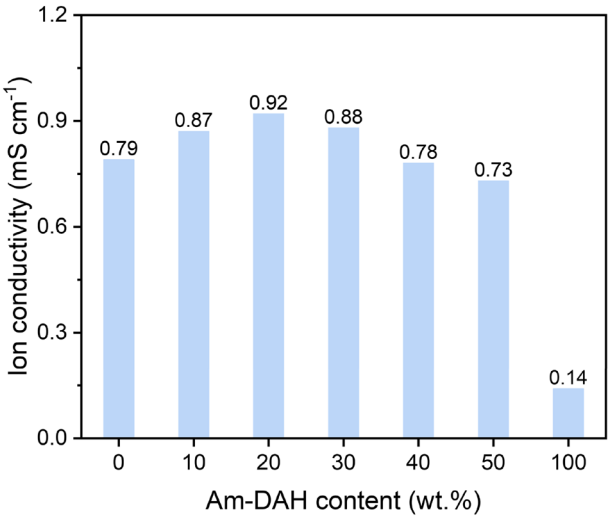

Supplementary Figure 3. The effect of Am-DAH content on the ionic conductivity of p(DAH-co-Am-DAH).

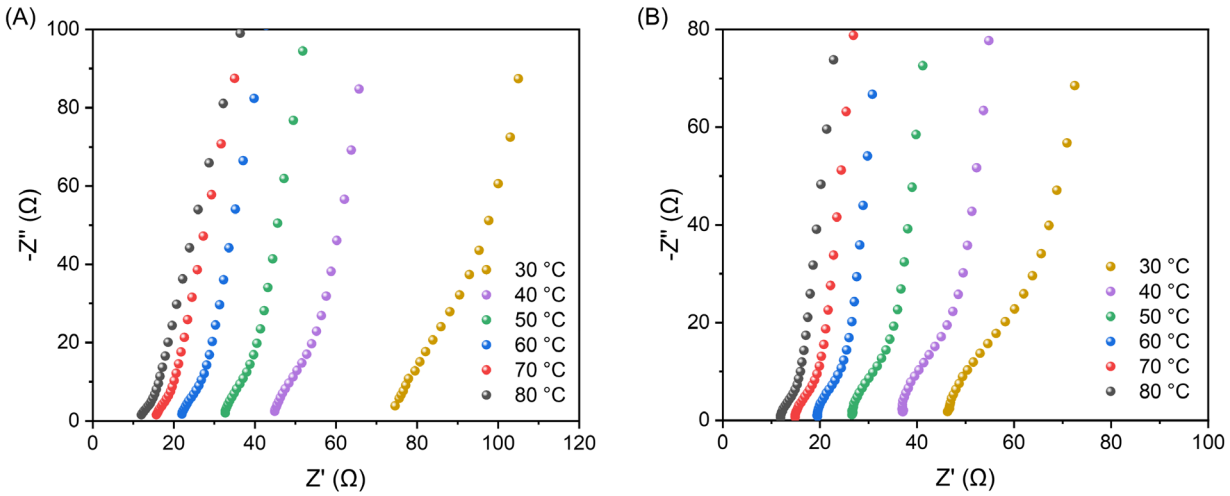

Supplementary Figure 4. Nyquist plots of (A) p(DAH) and (B) p(DAH-co-Am-DAH) from 30 to 80 ℃.

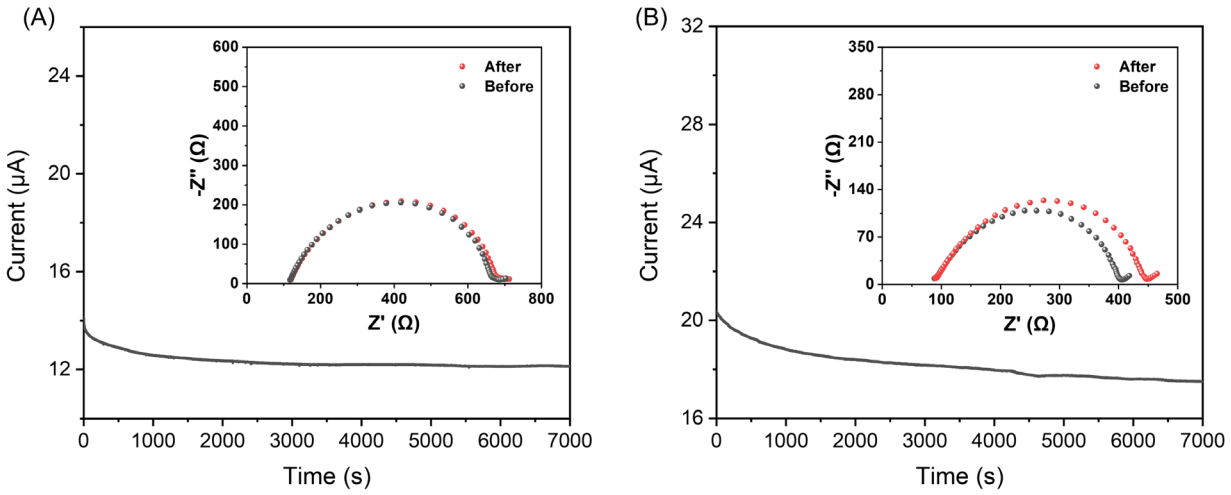

Supplementary Figure 5. *i*-t curves and Nyquist plots of (A) Li|p(DAH)|Li and (B) Li|p(DAH-co-Am-DAH)|Li at 30 ℃.

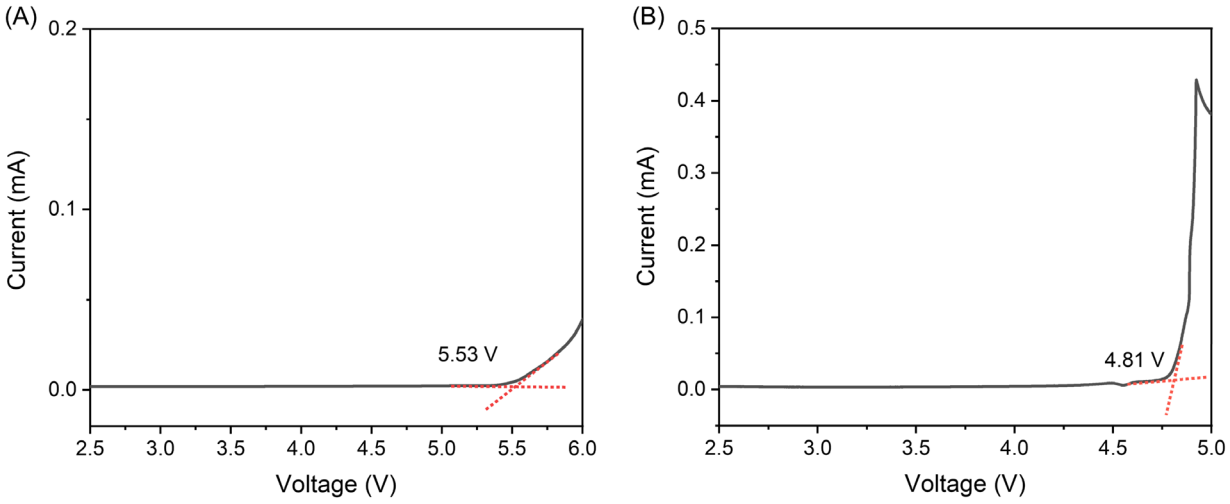

Supplementary Figure 6. LSV curves of (A) p(DAH) and (B) p(DAH-co-Am-DAH).

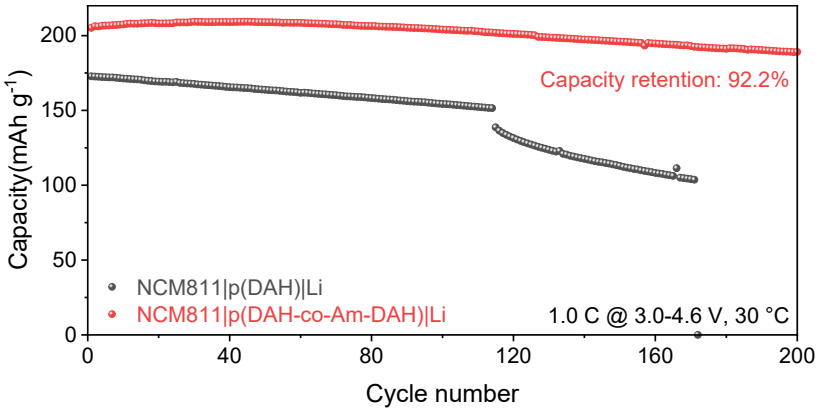

Supplementary Figure 7. Cycling performance of Li|p(DAH-co-Am-DAH)|NCM811 and Li|p(DAH)|NCM811.

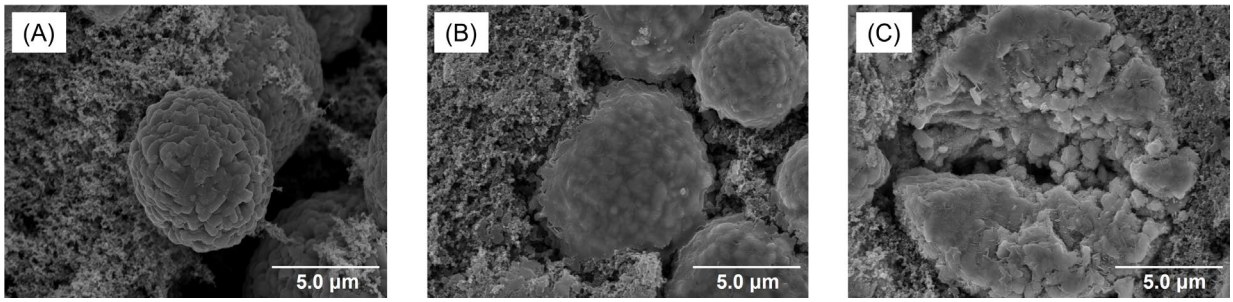

Supplementary Figure 8. SEM images of NCM811 cathode: (A) before cycling; (B) after 100 cycles at 2.8-4.6 V in Li|p(DAH-co-Am-DAH)|NCM811; (C) after 100 cycles at 2.8-4.6 V in Li|p(DAH)|NCM811.

As shown in Supplementary Figure 8, significant differences are observed in the surface morphology of the NCM811 cathodes after 100 cycles. The NCM811 particles cycled with the p(DAH-co-Am-DAH) electrolyte maintained excellent structural integrity, with their surfaces covered by a uniform coating layer, indicating the formation of a protective cathode electrolyte interphase.

Supplementary Table 1. Comparison of the battery performance of Li|p(DAH-co-Am-DAH)|NCM811 with that of other SPEs reported in the literature.

SPE materials	Initial discharge capacity (mAh g^{-1})	Cycle number	Capacity retention	Reference
p(DAH-co-Am-DAH)	**187.3 @ 1.0 C**	**200 @ 30°C** **350 @ 30°C** **500 @ 30°C**	**99.9%** **92.9%** **85.3%**	**This work**
FE18N	177.5 @ 1.0 C	200 @ 30°C	79.2%	[1]
BPMF-QSPE	190.4 @ 1.0 C	440 @ 25°C	70.1%	[2]
MTGPE	179.2 @ 1.0 C	260 @ 25°C	87.6%	[3]
FEGPE	167.0 @ 1.0 C	500 @ 25°C	75.0%	[4]
PPUM-PE	176.1 @ 0.5 C	250 @ 25°C	85.5%	[5]
$M_{3-x}PVH$	168.2 @ 0.5 C	300 @ 25°C	61.34%	[6]
MB-GPE	157.0 @ 0.5 C	400 @ 25°C	80.1%	[7]
PTFM	- @ 0.5 C	280 @ 25°C	75.6%	[8]
PPBB	152.4 @ 0.5 C	200 @ 25°C	80.0%	[9]
FL_7M_3@CSPESO	179.8 @ 0.5 C	95 @ 25°C	82.2%	[10]
Li-HA-F CSE	146.0 @ 0.5 C	500 @ 25°C	66.7%	[11]

References

1. Zhao, C.; Lu, Y.; Yan, K.; et al. Tailoring the chemical/electrochemical response in a quasi-solid polymer electrolyte enables the simultaneous in situ construction of superior cathodic and anodic interfaces. *Adv. Energy Mater.* **2024**, *14*, 2304532. DOI: 10.1002/aenm.202304532
2. Li, C.; Zhong, Y.; Liao, R.; et al. Robust and antioxidative quasi-solid-state polymer electrolytes for long-cycling 4.6 V lithium metal batteries. *Adv. Mater.* **2025**, *37*, 2500142. DOI: 10.1002/adma.202500142
3. Miao, X.; Hong, J.; Huang, S.; et al. In situ gel polymer electrolyte with rapid Li^+ transport

channels and anchored anion sites for high-current-density lithium-ion batteries. *Adv. Funct. Mater.* **2025**, *35*, 2411751. DOI: 10.1002/adfm.202411751

4. Chen, X.; Chu, F.; Li, D.; Si, M.; Liu, M.; Wu, F. In situ polymerized fluorine-free ether gel polymer electrolyte with stable interface for high-voltage lithium metal batteries. *Adv. Funct. Mater.* **2025**, *35*, 2421965. DOI: 10.1002/adfm.202421965
5. Wang, Y.; Zhang, S.; Chen, Z.; et al. Long-life lithium metal batteries enabled by in situ solidified polyphosphoester-based electrolyte. *Adv. Mater.* **2026**, *38*, e14210. DOI: 10.1002/adma.202514210
6. Xue, Y.; He, L.; Luo, D.; Dou, H.; Chen, Z. Oxygen vacancy nanowires regulate the continuous transport pathways and customized ionic microenvironment of solid-state electrolytes for stable lithium metal batteries. *Adv. Funct. Mater.* **2025**, *35*, 2509717. DOI: 10.1002/adfm.202509717
7. Zhang, S.J.; Li, Z.P.; Zhang, Y.X.; et al. Moderate Li^+-solvent binding for gel polymer electrolytes with stable cycling toward lithium metal batteries. *Energy Environ. Sci.* **2025**, *18*, 3807-3816. DOI: 10.1039/d4ee05866f
8. Zhang, Q.; Bian, T.; Wang, X.; Shi, R.; Zhao, Y. Unlocking mechanism of anion and cation interaction on ion conduction of polymer based electrolyte in metal batteries. *Angew. Chem. Int. Ed.* **2025**, *64*, e202415343. DOI: 10.1002/anie.202415343
9. Tao, F.; Yan, K.; Dong, C.; et al. Electric-dipole coupling ion-dipole engineering induced rational solvation-desolvation behavior for constructing stable solid-state lithium metal batteries. *Angew. Chem. Int. Ed.* **2025**, *64*, e202503037. DOI: 10.1002/anie.202503037
10. Jiang, Y.; Liu, L.; Liu, Y.; et al. A novel orientation aliphatic ketone-based liquid crystal polymer electrolyte for high-voltage solid-state lithium metal batteries. *Adv. Funct. Mater.* **2025**, *35*, 2502613. DOI: 10.1002/adfm.202502613
11. Peng, J.Y.; Lu, D.W.; Wu, S.Q.; et al. Lithium superionic conductive nanofiber-reinforcing high-performance polymer electrolytes for solid-state batteries. *J. Am. Chem. Soc.* **2024**, *146*, 11897-11905. DOI: 10.1021/jacs.4c00882